

Performance of wave function and Green’s function methods for non-equilibrium many-body dynamics

Cian C. Reeves,¹ Gaurav Harsha,² Avijit Shee,³ Yuanran Zhu,⁴ Chao Yang,⁴ K Birgitta Whaley,^{3,5} Dominika Zgid,^{2,6} and Vojtěch Vlček^{7,8}

¹*Department of Physics, University of California, Santa Barbara, Santa Barbara, CA 93117*

²*Department of Chemistry, University of Michigan, Ann Arbor, Michigan 48109, USA*

³*Department of Chemistry, University of California, Berkeley, USA*

⁴*Applied Mathematics and Computational Research Division,*

Lawrence Berkeley National Laboratory, Berkeley, CA 94720, USA

⁵*Berkeley Center for Quantum Information and Computation, Berkeley*

⁶*Department of Physics, University of Michigan, Ann Arbor, Michigan 48109, USA*

⁷*Department of Chemistry and Biochemistry, University of California, Santa Barbara, Santa Barbara, CA 93117*

⁸*Department of Materials, University of California, Santa Barbara, Santa Barbara, CA 93117*

(Dated: May 15, 2024)

Theoretical descriptions of non-equilibrium dynamics of quantum many-body systems essentially employ either (i) explicit treatments, relying on truncation of the expansion of the many-body wavefunction, (ii) compressed representations of the many-body wavefunction, or (iii) evolution of an effective (downfolded) representation through Green’s functions. In this work, we select representative cases of each of the methods and address how these complementary approaches capture the dynamics driven by intense field perturbations to non-equilibrium states. Under strong driving, the systems are characterized by strong entanglement of the single particle density matrix and natural populations approaching those of a strongly interacting equilibrium system. We generate a representative set of results that are numerically exact and form a basis for critical comparison of the distinct families of methods. We demonstrate that the compressed formulation based on similarity-transformed Hamiltonians (coupled cluster approach) is practically exact in weak fields and, hence, weakly or moderately correlated systems. Coupled cluster, however, struggles for strong driving fields, under which the system exhibits strongly correlated behavior, as measured by the von Neumann entropy of the single particle density matrix. The dynamics predicted by Green’s functions in the (widely popular) *GW* approximation are less accurate but improve significantly upon the mean-field results in the strongly driven regime.

INTRODUCTION

The properties of non-equilibrium quantum systems have drawn great attention in recent years. Driving a system can alter its properties, leading to phase changes[1, 2], exotic states of matter[3, 4] and allowing for tuning of material properties through continuous driving[5, 6]. Motivated by new experimental techniques and observations, the theoretical study of these non-equilibrium systems is also attracting wide attention[7–13]. This has led to a wide range of theoretical techniques, that have found success for equilibrium problems, to be extended to the non-equilibrium regime. The available ab-initio techniques that are systematically improvable either employ wave function or many-body Green’s function[14] as the basis of their solution. The former are typically used in quantum chemistry, while the latter is a suitable framework for condensed matter physics problems. There is however lack of critical assessment of their most appropriate domain applicability across various non-equilibrium regimes. While these approaches are, to a large extent, complementary formulations of the time dependent problem, they practically tackle the many-body description differently and hence face distinct challenges which are explored in this paper.

Among wave function methods, the time dependent exact diagonalization (TD-ED) is equivalent to the time evolution of the Schrödinger equation and hence it provides benchmark results. Due to its cost, it is applicable to only small finite systems. In the quantum chemistry community, it is referred to as time dependent full configuration interaction (TD-FCI)[15]. The time dependent methods based on an approximate (truncated) CI expansion enjoy much success, for example, time-dependent configuration interaction singles (TD-CIS) [16] method is very well suited for ionization dynamics. However, such methods have very limited applications, and active space-based CI methods are often preferred. One of the methods in that direction is the extension of multi-configurational time dependent Hartree approaches (MCTDH) [17] to atomic problems such as ionization of helium [18]. Several other methods in the same vein are also known, such as the time-dependent restricted active space CI (TD-RASCI) [19], and the complete active space self-consistent field (TD-CASSCF) [20]. The computational cost of those techniques scales exponentially with the size of the Hilbert space, each particular formulation has a different scaling prefactor, but are generally limited to small systems.

The reduced (non-exponential) scaling wavefunction-

based approaches leverage some form of compressed representation, e.g., as time dependent density matrix renormalization group method (TD-DMRG) [21–24] or time dependent formulation of coupled cluster [25, 26] (TD-CC) methods. For these approaches, the price of the reduction in computational scaling comes with the establishment of the domain of most suitable applicability. TD-DMRG is usually most successful in 1D systems, while TD-CC, following the ground-state version, is typically suitable for a wide variety of weakly correlated problems. [27–30] One of the earliest formulations of TD-CC, of particular interest to this work, was proposed by Arponen [7]. In recent years, new developments in theory and implementation have emerged. [31–34]

In contrast to the wavefunction methods, the methods applied to condensed matter systems are most conveniently based upon the Green’s function (GF) formulation of the many-body perturbation theory (MBPT)[35–37]. This approach recasts the many-body problem onto a set of effective correlators, most typically the one-quasiparticle GF[38], capturing the probability amplitude associated with the propagation of a quasiparticle. As an effective single particle quantity, GF MBPT can be efficiently implemented[39, 40] treating systems with thousands of electrons [41–43]. The complexity is accounted for via the space-time nonlocal self-energy that is systematically built by expansion in the system fluctuations[44–46], making GF MBPT one of the most powerful methods for studying electronic phenomena in large scale systems. It is formally straightforward to extend GF MBPT to non-equilibrium settings via the set of integrodifferential Kadanoff-Baym equations (KBEs)[47–49]. The cost of solving KBEs scales cubically with the number of timesteps[50]. Multiple cost reduction schemes have been proposed recently[51–58]. Yet, the most widely used of these is the Hartree-Fock generalized Kadanoff-Baym ansatz (HF-GKBA)[55] which can be formulated in linear scaling fashion[56, 59–62]. In some cases the HF-GKBA can even improve on elements of the KBEs, specifically the tendency of the KBEs to be overdamped and reach artificial steady states[63, 64].

In this paper, we critically compare the distinct formulations of the time dynamics and illustrate their performance on a series of numerical benchmarks for a generalized Hubbard chain driven out of equilibrium by an external pulse. Using TD-CI, TD-CC, the KBEs, the HF-GKBA and time dependent Hartree-Fock(TD-HF), we study the dynamics of the density matrix and study the effects of different strengths of non-equilibrium perturbation. In general, the TD-CI results serve as near-exact baseline against which other methods are compared.

The paper first reviews the essential parts of the distinct formulations and approximations in the theory section. The results then summarize the findings for lattice problems perturbed by pulses of increasing strengths that drive the system towards the regime which is shown to

exhibit characteristics of strong correlations. We map the capacity of the distinct formalisms to capture the dynamics for those regimes and also for systems with short- and long-range interactions, with and without non-local memory effects (in the context of GF formalisms), and confirm our findings by testing systems of various sizes. The details of the theory and implementation of the methods are in the supplementary information[65], while the main text focuses on the analysis of the results, which are summarized in the conclusion section.

THEORY

In this work, we explore representative formulations of three conceptually distinct methodologies, configuration interactions (based on truncation of the wavefunction expansion in the space of configurations represented by determinants), coupled cluster approach (employing the compression of the many-body wavefunction), and many-body Green’s function techniques (based on a downfolded effective representation of excitation evolution). In the following subsections we present the key underlying ideas and we leave much of the technical details of each approach to the supplemental information[65].

Time-dependent configuration interaction

The time dependent full configuration interaction (TD-FCI) approach is taken as a reference point for assessing the performance of the other methods. In TD-FCI, we express the time-dependent Schrödinger equation in configuration space:

$$i\frac{\partial C_I}{\partial t} = \sum_J H_{IJ}(t)C_J \quad (1)$$

where, I and J stand for all electronic configurations generated for a given problem, and C_I and C_J are the coefficients of those configurations. To solve this equation for a general time-dependent Hamiltonian we numerically implement the time-ordering and exponential of a large matrix, H_{IJ} , based on the Lanczos technique [66]. With this approach, we construct a propagator in a small subspace based on a reference form of the wavefunction at time t , i.e., $|\Psi(t)\rangle$. For example, at $t = t_0$, we build a propagator based on the ground state wave function of the time-independent Hamiltonian. Such a propagator is however valid only for a short time. Through a regular renewed search of the “active” subspace we can ultimately propagate the TD-FCI expansion for long times. The procedure is numerically stable and yields unitary dynamics; the details of the implementation are provided in the supplemental information[65].

Time-dependent coupled cluster

Coupled cluster (CC) is another formalism expanding the wavefunction as a linear combination of configurations. In CC, one introduces a non-Hermitian approximation to expectation values $\langle A \rangle_{CC} = \langle \Psi_L | A | \Psi_R \rangle$, where the bra and ket wavefunctions are defined as

$$|\Psi_R\rangle = e^T |\Phi\rangle, \quad (2a)$$

$$\langle \Psi_L | = \langle \Phi | (1 + Z) e^{-T}, \quad (2b)$$

where $T = \sum_{\mu} \tau_{\mu} \gamma_{\mu}^{\dagger}$ and $Z = \sum_{\mu} z_{\mu} \gamma_{\mu}$ are composed of particle-hole excitation γ_{μ}^{\dagger} and de-excitation γ_{μ} operators, defined with respect to the Slater determinant reference $|\Phi\rangle$.

In time-dependent CC, the amplitudes τ_{μ} and z_{μ} carry all the time-dependence, and are found by making the action integral,

$$\begin{aligned} S &= \int dt \mathcal{L}(t) \\ &= \int dt \langle \Phi | (1 + Z(t)) e^{-T(t)} \left(i \frac{\partial}{\partial t} - H(t) \right) e^{T(t)} | \Phi \rangle, \end{aligned} \quad (3)$$

stationary with respect to variations in $\tau_{\mu}(t)$ and $z_{\mu}(t)$. When no truncation is imposed on the operators T and Z , CC is equivalent to exact diagonalization, i.e., equivalent to FCI (discussed above) where the wavefunction is constructed as a linear combination of all possible Slater determinants within the given spin-orbital basis. In practice, however, truncation is necessary. Fortunately, in weak-to-moderately correlated systems, it is sufficient to include only single and double particle-hole excitation (de-excitation) operators in T (Z). This leads to the well known CCSD approximation which is used for all the results and discussion presented in this paper.

It is noteworthy that due to the exponential parameterization, the ket wavefunction in truncated CC includes contributions from all Slater determinants, although these contributions are factorized in terms of the lower-rank parameters. This is in contrast with truncated CI, where the cut-off is imposed explicitly on the number of determinants. At the same time, the asymmetric nature of CC expectation values leads to a violation of the variational principle. Consequently, in TD-CC, real observable quantities may develop un-physical or complex parts. However, the unphysical terms often serve as a diagnostic tool for the CCSD approximation. In the moderately interacting regimes, where CC works well, the expectation values are well behaved. The increasing magnitude of unphysical expectation values generally coincides with the onset of strong correlations, where CC is known to fail. This point will be discussed in the sections below. Further details regarding the derivation and implementation of the TD-CC equations are provided in the supplemental information. [65]

Green's function methods

Finally we employ two approaches based on the time evolution of the one-particle Green's function (GF), i.e., the time dependent probability amplitude associated with propagation of a quasiparticle. At non-equilibrium, the GF is an explicit function of two time arguments, and their respective ordering on the real time axis (as well as imaginary time axis for the finite temperature formalisms). The first are the Kadanoff-Baym equations, representing a set of theoretically exact integro-differential equations for the two-time GF, and are given by[67]

$$\begin{aligned} [-\partial_{\tau} - h]G^M(\tau) &= \delta(\tau) + \int_0^{\beta} d\bar{\tau} \Sigma^M(\tau - \bar{\tau})G^M(\bar{\tau}), \\ i\partial_{t_1}G^{\uparrow}(t_1, -i\tau) &= h^{\text{HF}}(t_1)G^{\uparrow}(t_1, -i\tau) + I^{\uparrow}(t_1, -i\tau), \\ -i\partial_{t_2}G^{\uparrow}(-i\tau, t_2) &= G^{\uparrow}(-i\tau, t_2)h^{\text{HF}}(t_2) + I^{\uparrow}(-i\tau, t_2), \\ i\partial_{t_1}G^{\leq}(t_1, t_2) &= h^{\text{HF}}(t)G^{\leq}(t_1, t_2) + I_1^{\leq}(t_1, t_2), \\ -i\partial_{t_2}G^{\leq}(t_1, t_2) &= G^{\leq}(t_1, t_2)h^{\text{HF}}(t_2) + I_2^{\leq}(t_1, t_2), \end{aligned} \quad (4)$$

Here Σ is a space-time nonlocal effective potential embodying all many-body interactions; $G^{M, <, >, \uparrow, \downarrow}$ are various components of the Green's function that depend on which of the time arguments are in real time versus in imaginary time and the $I^{<, >, \uparrow, \downarrow}$ are integrals that account for many-body correlation effects in the system. A full description and discussion of these quantities is given in the supplemental information[65].

The KBEs are approximate only through the choice of the self-energy. In this work, we focus on the GW approximation, representing the arguably most popular choice for simulations of condensed matter systems. In essence, this approach accounts for dynamical density-density interactions, which dominate the correlation effects in weakly and moderately correlated systems (such as semiconductors[14, 44, 68]). The combination of integrals in the equations above and their two-time nature means solving the KBEs scales cubically in the number of time steps, making these calculations prohibitively expensive. Furthermore, the KBEs often suffer from issues of artificial damping coming from the approximate self-energy[63, 64].

Given the cost of KBEs propagation, they often solved only approximately, and the most common route is to employ the Hartree-Fock Generalized Kadanoff-Baym ansatz (HF-GKBA). It assumes a particular self-energy for the time diagonal component of the GF and takes the off-diagonal self-energy to be approximated by only the bare exchange interactions (hence the Hartree-Fock (HF) approximation in its name). By using the HF form of the time off-diagonals, it is possible to derive an ordinary differential equation (ODE) scheme for the evolution of the equal-time component of the GF. This translates to a

time-linear formalism that recasts the equation of motion using the explicit form of the two particle GF instead of making use of Σ [56, 69]. The equations of motion for this scheme are given by:

$$\begin{aligned} i\partial_t G_{ij}^<(t) &= [h^{\text{HF}}(t), G^<(t)]_{ij} + [I + I^\dagger]_{ij}(t), \\ I_{ij}(t) &= -i \sum_{klp} w_{iklp}(t) \mathcal{G}_{lpjk}(t), \\ i\partial_t \mathcal{G}_{ijkl}(t) &= [h^{(2),\text{HF}}(t), \mathcal{G}(t)]_{ijkl} \\ &\quad + \Psi_{ijkl}(t) + \Pi_{ijkl} - \Pi_{lkji}^*. \end{aligned} \quad (5)$$

Here $\mathcal{G}(t)$ is a two particle propagator, Ψ_{ijkl} accounts for pair correlations built up due to two-particle scattering events and Π_{ijkl} accounts for polarization effects[69]. While approximate, the HF-GKBA does not suffer from artificial damping as the KBEs do and thus in some cases offers improved results over the KBEs at a much reduced cost. This further enables the use of more advanced forms of Σ , the study of larger systems, and the ability to perform longer time evolution. A more detailed description of the HF-GKBA and the ODE scheme are given in the supplemental information[65].

Model Systems

To benchmark different time-dependent methods, we use a generalization of the one-dimensional Hubbard model, which is driven out of equilibrium with the help of an electric-field pulse. The Hamiltonian for the system is written as:

$$\begin{aligned} \mathcal{H} = -J \sum_{\langle i,j \rangle \sigma} c_{i\sigma}^\dagger c_{j\sigma} + U \sum_i n_{i\uparrow} n_{i\downarrow} \\ + V \sum_i (-1)^i n_i + \sum_{ij} h_{ij}^{\text{N,E}} c_i^\dagger c_j. \end{aligned} \quad (6)$$

The first two terms are the usual nearest neighbor hopping and onsite interaction of the Hubbard model. The third term turns the system into a bipartite lattice and serves to open up a trivial gap in the system. This is necessary since the HF-GKBA prepares the initial state using adiabatic switching. The adiabatic theorem requires a gapped system to correctly prepare the HF-GKBA initial state. Such gapped models have been used in previous studies of the HF-GKBA[57, 58]. We choose $J = 1$ and express all interaction strengths in units of J . Further, all the results and discussion assume half filling, i.e., one electron per site.

For each method the system is prepared in the corresponding ground state before being excited with a time dependent field modeled under the dipole approximation and given by

$$h_{ij}^{\text{N,E}}(t) = \delta_{ij} \left(\frac{N-1}{2} - i \right) E e^{-\frac{(t-t_0)^2}{2\sigma^2}}. \quad (7)$$

Here N is the number of lattice sites in the model, E is the strength of the field, σ determines the temporal width of the pulse and t_0 is the pulse midpoint.

RESULTS

Effect of excitation strength

First we investigate the effect of the strength of the perturbation by varying the parameter E in our model. This will capture the behavior of each method as we go from linear response type excitations up to strongly perturbed regimes. In Fig. 1 we show the dynamics of the electronic dipole for the system in equation (6) and (7) with $E = 1.0J, 2.0J, 3.0J$ and $5.0J$, as computed with each of our methods. For this section, we show results obtained for the number of sites $N = 12$ and we choose an interaction strength of $U = 1.0J$. This puts the kinetic and Coulomb energy scales at the same level. Here each method captures the $U = 1.0$ ground states very well. Thus, this setup allows us to see how each method performs in non-equilibrium without having to worry about the effects of a poorly captured ground state. While we have explored various parameters, the findings below are representative of the behaviors observed. Additional results are discussed in the supplemental information[65].

We will start this section by discussing the results produced by the reference TD-CI approach, which is numerically exact. These results will serve as our benchmark to compare against other methods. For $E = 1.0J$, we see two dominant types of oscillation: a strong low-frequency contribution that manifests as long wavelength oscillations in the dipole and a weak high-frequency contribution. This behavior continues with increasing E , however, for strong perturbation strengths, we see that the magnitude of both types of oscillations diminishes, and a yet lower frequency mode begins to dominate. This continues until the dynamics become almost flat when we come to the bottom panel of Fig. 1 with $E = 5.0J$. Further results and analysis to understand these exact trends in dipole moment are discussed in Sec. and .

We continue this section by comparing the results produced by our other methods.

For completeness, we include the TD-HF trajectory, which serves as a baseline for the types of expansion techniques discussed below (either CC or those based on the GFs, with HF being their underlying reference Hamiltonian around which the self-energy is expanded). TD-HF is based solely on a time evolution using a single determinant. For $E = 1.0J$ we see TD-HF performs well, capturing the amplitude and frequency of the oscillations of the TD-CI. It suffers from a similar issue the HF-GKBA has in that it has a slight offset in frequency that causes it to move out of phase with the exact result as the time evolution progresses. Interestingly for

$E = 2.0J$ the TD-HF actually improves upon the results given by HF-GKBA and the KBEs. This fortuitous improvement is likely due to the self-energy over-damping the MBPT results. As E is increased again we see the result worsen. For $E = 3.0J$ TD-HF is in agreement up to $t \approx 10J^{-1}$ and for $E = 5.0J$ to around $t = 8J^{-1}$. After these times however the TD-HF result differs drastically, although still oscillates around the correct result. Judging by the results, it seems now the TD-HF result is not damped enough, due to the lack of a self-energy and thus oscillates with much greater amplitude than the benchmark results. In the next paragraphs, we discuss the CC and GF-based techniques, which can be thought of as expansions around this “correlation-free” TD-HF dynamics.

The TD-CC approach is in excellent agreement with TD-CI for the lowest two E values ($E = 1.0J, 2.0J$). Note that this is despite the relatively complex dynamics. For increased strength (starting with $E = 3.0J$), TD-CC captures the dynamics very closely only up until $t \approx 10J^{-1}$, but deviates from the exact solution soon after. This illustrates a growing error in TD-CC for long-time evolutions at large excitation strengths despite the initial TD-CC dynamics for $E = 3.0J$ being in reasonable qualitative agreement with TD-CI. Note that without the TD-CI reference, it is not immediately clear from Fig. 1 that TD-CC dynamics is erroneous. For $E = 4.0J, 5.0J$, soon after the system is driven out of equilibrium (around $t \approx 5J^{-1}$), the CC approach starts to break down, and the results become unphysical as the occupation numbers develop a large imaginary contribution. In fact, the disagreement of CC with TD-CI in the presence of strong perturbation can be anticipated by looking at Fig. S6 of SI, [65] where we plot the imaginary part of CC estimates for the occupation number on the first site in the Hubbard lattice. It is evident that even for $E = 3.0J$ at long time scales, and especially for $E = 4.0J, 5.0J$, TD-CC leads to large unphysicalities, signaling its breakdown. At the same time, keeping track of imaginary parts or inconsistent behavior in expectation values in TD-CC can serve as a diagnostic tool to measure the efficacy of the coupled cluster approximation itself.

Next, we turn to the MBPT methods, starting with the solution for the KBEs using the GW self-energy. For $E = 1.0J$ the agreement is very strong up to $t \approx 15J^{-1}$. After this, while TD-CC improves in the quantitative results, the KBEs still provide qualitatively correct results. They capture the low frequency mode of oscillation extremely well, however the high frequency part is damped out almost entirely by $t \approx 25J^{-1}$. Moving to $E = 2.0J$, the time up to which we see perfect agreement is shortened to $t \approx 10J^{-1}$. Additionally, unlike the $E = 1.0J$ case where reasonable qualitative agreement held until $t = 50J^{-1}$, here we see that after $t \approx 20J^{-1}$ the KBE results differ significantly from those produced by TD-CI and TD-CC. The damping in the KBEs is more pro-

nounced now, and the dynamics are close to flat. This damping represents a well-known issue with the KBEs and will be discussed later in section . This trend continues as we continue to increase the excitation strength. For $E = 3.0J$, perfect agreement with TD-CI now only holds to $t \approx 10J^{-1}$, around the same as the TD-CC result. The KBE damping kicks in almost immediately after this at $t \approx 12J^{-1}$. After this the KBE dynamics are essentially flat. Interestingly, the exact TD-CI result seems to oscillate around the stationary value that the KBEs reach. For $E = 5.0J$ the KBE results fail almost immediately by strongly suppressing any oscillations at or after $t \approx 5J^{-1}$. Again, we see the result is damped (leading to only a slowly time-varying dipole moment which monotonically increases within the simulation window). However, compared to the TD-CI result, this is not *qualitatively* wrong despite the magnitude of the dipole is now much further from the TD-CI result compared to the results in Fig. 1(a)-(c).

We now turn to the HF-GKBA, which truncates certain memory effects compared to the KBEs. Similar to KBEs, we see an excellent agreement with TD-CI for $E = 1.0J$ up until $t \approx 15J^{-1}$. After this, the HF-GKBA still shows a strong qualitative and quantitative agreement compared to the benchmark results, contrasting with the overdamped behavior of KBEs. The HF-GKBA captures the low frequency mode of oscillation very well. For longer times, the high frequency oscillations from the TD-CI and TD-CC results are offset. Additionally, the magnitude of these high frequency oscillations is diminished relative to the benchmark results. However, the HF-GKBA does systematically improve on the damping seen in the KBE result. For $E = 2.0J$ the HF-GKBA follows a very similar trend to the KBEs. The main difference is, again, a reduction in the damping seen in the KBE dynamics. Both follow roughly the same trajectory, which appears to be centered around the main low frequency oscillations of TD-CI and TD-CC. Moving to $E = 3.0J$ the HF-GKBA result now has a noticeable offset from the KBE solution, but keeps the same trend of improving upon the overdamping. After $t \approx 10J^{-1}$ the HF-GKBA no longer captures the benchmark results qualitatively or quantitatively. Furthermore, the HF-GKBA oscillates minorly around a single value (somewhat similarly to the KBEs). However, the value the HF-GKBA result seems to center around is lower than the central values of the TD-CI, TD-CC, and the KBEs which are more or less equivalent. Turning finally to Fig. 1(d) with $E = 5.0J^{-1}$ we see the HF-GKBA actually captures the qualitative behavior of the TD-CI dipole well. The HF-GKBA displays a slightly larger magnitude of oscillation than those of TD-CI, however the mean values are very close and it offers a markedly significant improvement over the TD-CC and KBE results.

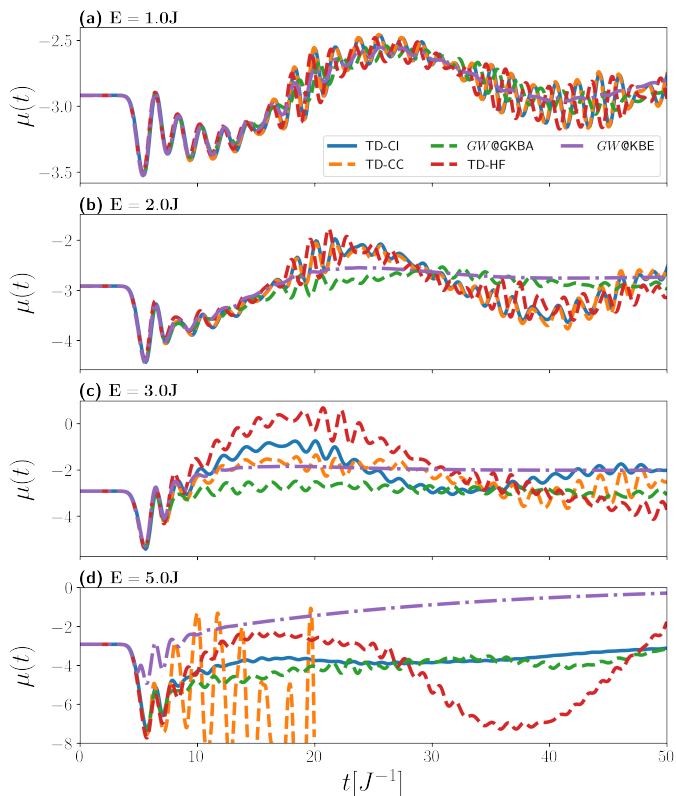


FIG. 1. Dynamics of the electronic dipole system described by Eq. (6) and (7) for various values of E parameter. a) $E = 1.0J$, b) $2.0J$, c) $3.0J$ d) $5.0J$.

Exciting to strongly correlated non-equilibrium regime

In this section, we further investigate the results discussed in section . As the TD-CI results provide access to the (nearly exact) wavefunction trajectory, we use it to analyze the time evolution in greater depth. In the next section (), we rely on this analysis to illustrate the origins of failure in each method in capturing the proper physics of non-equilibrium systems.

In Fig. 2(a)-(c), we show the natural occupations of the single particle density matrix for the model discussed in section and section for $E = 1.0J$, $E = 2.0J$ and $E = 5.0J$. The natural occupations correspond to the eigenvalues of time dependent single particle density matrix expressed in spin-orbitals, taken from TD-CI. Our analysis is motivated by equilibrium, ground-state physics of the underlying half-filled Hubbard model, where natural occupations approach $\lambda_i \rightarrow 0.5$ as the system becomes strongly correlated in the $U \rightarrow \infty$ limit (see Fig. S3 in supplemental information[65]). By examining natural occupations, one can therefore assess how correlated the system is. Here we propose this quantity as a measure of correlation in the non-equilibrium setting.

In Fig. 2 (d), we also look at the von-Neumann entropy

for a scan of E values from $1.0J$ to $5.0J$. The entropy is computed as,

$$S[\rho] = \frac{2}{N} \text{Tr} [\rho \log_2(\rho)]. \quad (8)$$

Note that for the ground-state, as $U \rightarrow \infty$, the entropy approaches unity.

For $E = 1.0J$, in Fig. 2(a), we see very little deviation from the natural occupations. This corresponds to near zero entropy of the single particle density matrix. Each of our methods matches the benchmark perfectly in equilibrium for the results in Fig 1. This demonstrates that when the natural occupations remain close to the equilibrium values the four methods capture well the non-equilibrium TD-CI results qualitatively and even quantitatively.

As the excitation strength is increased to $E = 2.0J$, we see a more noticeable difference from the equilibrium result. Though the oscillations of the natural occupations are still relatively small. The entropy reflects this more clearly where it is only around $S[\rho] = 0.1$, indicating weak mixing between the natural orbitals. For the dynamics in Fig. 1, the results produced by TD-CC are still in perfect agreement with the TD-CI result. For the same conditions, the MBPT methods appear over damped but they still capture elements of the TD-CI result.

For $E = 5.0J$ we see a strong mixing of the natural occupations, nearing the $\lambda_i[\rho] = 0.5$ limit, corresponding to an entropy of $S[\rho] \approx 0.9$. In an equilibrium picture this would correspond to a strongly correlated system, with high U . Such a transition was observed for all system sizes and interaction range types. Consequently, we consider this to be a representative case of a system driven by a strong external perturbation from a “weakly correlated” ground state to a “strongly correlated” excited state.

Understandably, such a physical regime poses difficulty for methods suited for weakly correlated systems, such as CC or the MBPT expansion. Indeed, TD-CC results fail completely in this regime, as do the KBE results. In contrast the HF-GKBA offers an improvement in this regime and does a good job at capturing qualitative and quantitative of the TD-CI results. In Fig. S5 of the supplemental information we show the entropy for different E for $N_s = 8, 12$ and 16 and see similar behavior for each system size[65].

DISCUSSION AND CONCLUSIONS

We now return to discuss the implications of the results we have described in section and . Each of the methods we test perform reasonably well in weakly excited systems. For pulse strengths up to $E = 2.0J$ TD-CC gives perfect agreement compared to TD-CI. However, as stronger perturbations are applied to drive the sys-

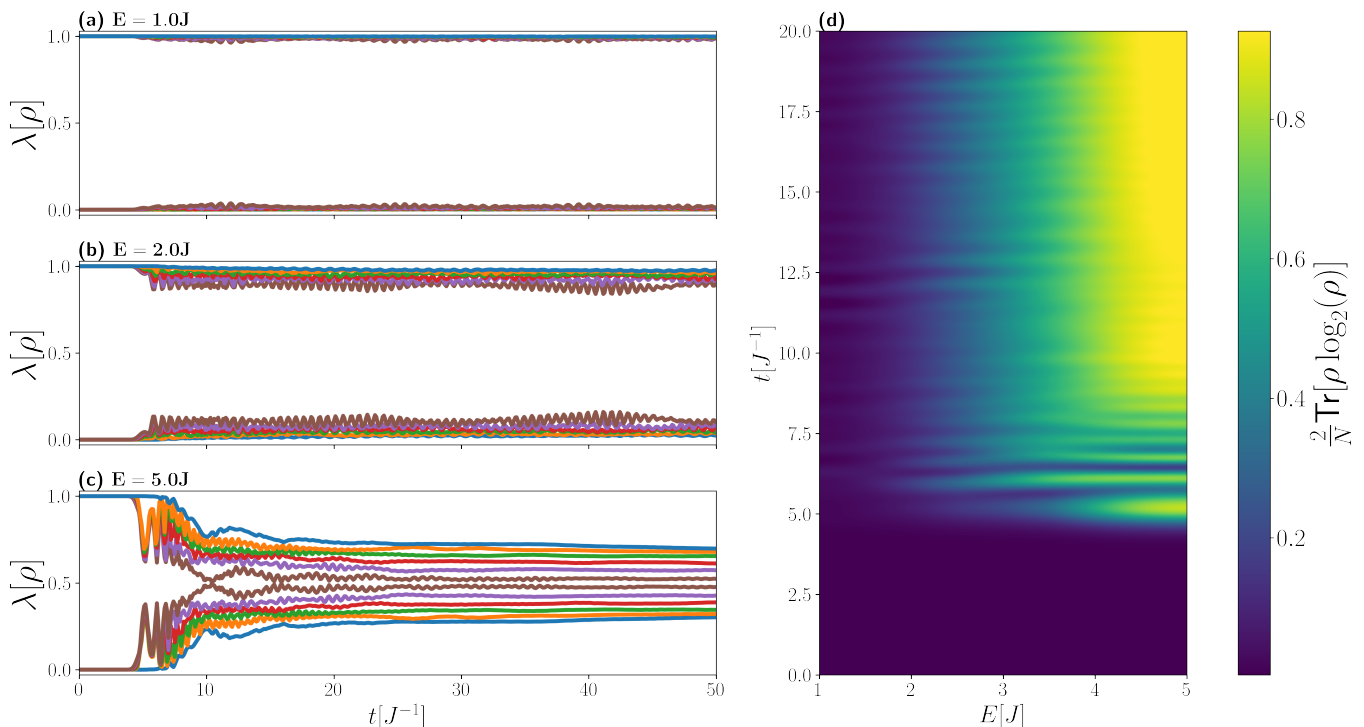


FIG. 2. *Left*: Natural occupations of the single particle density matrix taken from TD-CI for the model discussed in section and section for a) $E = 1.0J$, b) $E = 2.0J$ and c) $E = 5.0J$. *Right*: The entropy for a scan of E values from $1.0J$ to $5.0J$

tem out of equilibrium, TD-CC breaks down. This is because CC wavefunction is expanded around the time-independent, ground-state Hartree-Fock reference which becomes increasingly bad as the system evolves after a strong time-dependent perturbation.

Although, even for $E = 3.0J$ TD-CC offers a good improvement over the HF-GKBA and the KBEs. Interestingly, at $E = 2.0J$ we observe that TD-HF also improves upon the results for the time-dependent dipole produced by HF-GKBA and the KBEs. Note that this implies that the trajectories of equal-time observables depending on the density matrix (such as the dipole studied here) are qualitatively well captured even by a mean-field technique. Further, this leads to the interesting question of whether in dynamical systems it is always better to include self-energy effects, or whether there are regimes in which the inclusion of the (non-exact) self-energy can have detrimental effects by overdamping the system dynamics. This is a question that deserves further investigation with additional forms of the self-energy beyond merely the density-density response included in the GW formalism, but also including higher order fluctuations[45, 46].

In the $E = 1.0J$ case the Kadanoff-Baym equations qualitatively capture the dynamics after excitation. However, as is commonly seen[63, 64] they suffer from severe overdamping that removes the high frequency component of the dipole almost immediately. For $E = 1.0J$

the HF-GKBA also captures the qualitative features of the dipole oscillations and even offers improvement to the KBEs by removing some of the damping. As we increase E further, the full KBEs continue to be overdamped, while the HF-GKBA improves the result, adding back in some of the high frequency oscillation modes lost in the KBEs.

Interestingly, as we show in Fig. S4 of the supplemental information[65], when long range interactions are included in the Hamiltonian the result of the HF-GKBA are improved *drastically*. This improvement is likely related to the suitability of a self-energy approximation for a given problem. The GW approximation, used here, assumes the dominant contribution to the self-energy is from the screened coulomb interaction, or equivalently from the induced charge density fluctuations. Due to the extremely localized nature of the Hubbard model screening is relatively weak, meaning a different self-energy approximation may be more appropriate. A long range interacting model naturally has more potential for screening, thus making the GW approximation a more relevant contribution to the self-energy, and so improving the agreement with TD-CI.

This observation may also help to explain the improvement of the HF-GKBA for $E = 5.0J$. In this highly excited regime, the particles are much more delocalized. This increases the screening and we propose that this lead to a regime in which the physics accounted for by

the *GW* approximation becomes more dominant, leading to reasonably well captured dynamics. Indeed, *GW* can be interpreted as dynamically screened exchange interaction, i.e., its difference compared to TD-HF stems purely from adding correlations effects due to the density fluctuations which likely dominate in this regime, over other types of correlations. It is in this regime that CC shows its most significant failing, showing results that are drastically different from the CI result both quantitatively and qualitatively. Here, the main difference between GF MBPT and CC stems from resummations of the screened interactions, which are not included in CC. TD-CC can possibly be improved via orbital optimization in the pursuit of renormalizing the interactions, as well as by including additional higher-order excitation terms (beyond the CCSD level).[31–33, 70]

From these results, it is clear that the TD-CC performs excellently for relatively weak perturbations and improves upon MBPT, especially in the finer details. However, in strongly perturbed regimes, TD-CC breaks down and no longer provides results that match TD-CI, even at the qualitative level. Notably, for regimes in which the system is strongly perturbed, the HF-GKBA offers results that are very close to those produced by TD-CI, and are much more numerically stable than those produced by TD-CC. This points to the possibility that the HF-GKBA and TD-CC have somewhat complimentary regimes of applicability, however definitive statements about this observation will require further exploration of various self-energy formulations. As is often seen the KBEs show no significant improvement upon the HF-GKBA, furthermore in this particular example due to the severe overdamping the HF-GKBA outperforms the KBEs. This points to the fact that inclusion of the time-nonlocal components of the self-energy, which dominate the “quantum memory” of KBEs, is practically detrimental to the quality of the predicted dynamics, despite its formal correctness. This question warrants further exploration, especially in connection to applications of more involved self-energy formulations, beyond *GW*.

We link the observed performance of the CC and GF methods (within the given approximations) to the effective strength of correlations induced by the non-equilibrium. In section , we looked at the different regimes brought about by varying the pulse strength. The entropy of the density matrix, given in equation (8), is here used to quantify correlations in the system[71]. In Fig. 2 we showed that for stronger pulses the natural populations become closer to $\lambda = 0.5$, which is consistent with those of a strongly interacting equilibrium system as shown in Fig. S3 of the supplemental information for the model in equation (6) with $N_s = 6$ [65]. Further, in in Fig. 1 (d) the dynamics of the dipole are very slowly varying in time. This is consistent with the type of dynamics one would see in a very strongly interacting system due suppression of the kinetic energy term. We interpret this

regime as non-equilibrium induced correlations.

In this work we have only investigated properties related to the density matrix, namely the dipole and the von Neumann entropy. Capturing the dynamics of the density matrix is an important benchmark for any time dependent method, and being able to predict these quantities is valuable for quantitative simulation of carrier dynamics in materials or charge dynamics in quantum chemistry systems. On the other hand, other measurable quantities of great importance for non-equilibrium quantum physics, such as the the time-dependent spectral function, require knowledge of the time-non-local terms. We are actively investigating the ability of each of these methods to capture the time dependent spectral properties of non-equilibrium systems, as well as looking into efficient ways of improving existing approaches[72].

A further extension of this study, also underway, comes in terms of the system sizes studied. Despite the huge reduction in cost afforded in TD-CI compared to full diagonalization, we are still limited in the system size due to the still large size of the constructed subspace. One route we are actively pursuing is implementing a time dependent adaptive sampling CI approach(TD-ASCI). This approach improves upon traditional CI by adding a step that weights wavefunctions making up the subspace, based on estimating how much of a contribution they will make to the subspace. This can vastly reduce the subspace size thus opening the road to even larger systems. This presents a route to provide accurate benchmark data in large scale or multi-band periodic systems where such data is extremely difficult to obtain.

In conclusion, the numerical benchmarks presented in this work help to practically assess the performance of variety of time-dependent numerical methods under different strengths of perturbation. We demonstrate that TD-CC is an excellent theory for moderate coupling and weak to moderately strong perturbations, but that it becomes unreliable for strong perturbations. We have further seen the KBEs fail to produce results that improve upon TD-CC. For weak excitations the HF-GKBA produces worse results than TD-CC but for strong excitations the HF-GKBA gives results that are qualitatively and quantitatively very close to the true result. Thus, we surmise that a multilayered methodology employing the complementary strengths of TD-CC and HF-GKBA will likely provide accurate results in a wide variety of non-equilibrium regimes.

ACKNOWLEDGEMENTS

This material is based upon work supported by the U.S. Department of Energy, Office of Science, Office of Advanced Scientific Computing Research and Office of Basic Energy Sciences, Scientific Discovery through Advanced Computing (SciDAC) program under Award

Number DE-SC0022198. This research used resources of the National Energy Research Scientific Computing Center, a DOE Office of Science User Facility supported by the Office of Science of the U.S. Department of Energy under Contract No. DE-AC02-05CH11231 using NERSC award BES-ERCAP0029462

-
- [1] M. R. Beebe, J. M. Klopff, Y. Wang, S. Kittiwatanakul, J. Lu, S. A. Wolf, and R. A. Lukaszew, Time-resolved light-induced insulator-metal transition in niobium dioxide and vanadium dioxide thin films, *Opt. Mater. Express* **7**, 213 (2017).
- [2] A. S. Disa, J. Curtis, M. Fechner, A. Liu, A. von Hogen, M. Först, T. F. Nova, P. Narang, A. Maljuk, A. V. Boris, B. Keimer, and A. Cavalleri, Photo-induced high-temperature ferromagnetism in YTiO₃, *Nature* **617**, 73 (2023).
- [3] S. Dong, M. Puppini, T. Pincelli, S. Beaulieu, D. Christiansen, H. Hübener, C. W. Nicholson, R. P. Xian, M. Dendzik, Y. Deng, Y. W. Windsor, M. Selig, E. Malic, A. Rubio, A. Knorr, M. Wolf, L. Rettig, and R. Ernstorfer, Direct measurement of key exciton properties: Energy, dynamics, and spatial distribution of the wave function, *Natural Sciences* **1**, e10010 (2021).
- [4] C. Bao, P. Tang, D. Sun, and S. Zhou, Light-induced emergent phenomena in 2D materials and topological materials, *Nature Reviews Physics* **4**, 33 (2022).
- [5] M. Nuske, L. Broers, B. Schulte, G. Jotzu, S. A. Sato, A. Cavalleri, A. Rubio, J. W. McIver, and L. Mathey, Floquet dynamics in light-driven solids, *Phys. Rev. Res.* **2**, 043408 (2020).
- [6] S. Zhou, C. Bao, B. Fan, F. Wang, H. Zhong, H. Zhang, P. Tang, W. Duan, and S. Zhou, Floquet engineering of black phosphorus upon below-gap pumping, *Phys. Rev. Lett.* **131**, 116401 (2023).
- [7] J. Arponen, Variational principles and linked-cluster expansion for static and dynamic many-body problems, *Annals of Physics* **151**, 311 (1983).
- [8] K. L. Ishikawa and T. Sato, A Review on Ab Initio Approaches for Multielectron Dynamics, *IEEE Journal of Selected Topics in Quantum Electronics* **21**, 1 (2015).
- [9] X. Li, N. Govind, C. Isborn, A. E. DePrince, and K. Lopata, Real-Time Time-Dependent Electronic Structure Theory, *Chem. Rev.* **120**, 9951 (2020).
- [10] J. Sun, C.-W. Lee, A. Kononov, A. Schleife, and C. A. Ullrich, Real-Time Exciton Dynamics with Time-Dependent Density-Functional Theory, *Phys. Rev. Lett.* **127**, 077401 (2021).
- [11] D. Karlsson, R. van Leeuwen, Y. Pavlyukh, E. Perfetto, and G. Stefanucci, Fast Green's Function Method for Ultrafast Electron-Boson Dynamics, *Phys. Rev. Lett.* **127**, 036402 (2021).
- [12] E. Perfetto, Y. Pavlyukh, and G. Stefanucci, Real-Time GW: Toward an ab initio description of the ultrafast carrier and exciton dynamics in two-dimensional materials, *Phys. Rev. Lett.* **128**, 016801 (2022).
- [13] B. Sverdrup Ofstad, E. Aurbakken, Ø. Sigmundson Schøyen, H. E. Kristiansen, S. Kvaal, and T. B. Pedersen, Time-dependent coupled-cluster theory, *WIREs Computational Molecular Science* **13**, e1666 (2023).
- [14] R. M. Martin, L. Reining, and D. M. Ceperley, *Interacting electrons* (Cambridge University Press, 2016).
- [15] Note, that in ED the system Hamiltonian is diagonalized providing all the eigenvectors, while in TD-FCI customarily only few eigenvectors are obtained.
- [16] N. Rohringer, A. Gordon, and R. Santra, Configuration-interaction-based time-dependent orbital approach for ab initio treatment of electronic dynamics in a strong optical laser field, *Phys. Rev. A* **74**, 043420 (2006).
- [17] A. U. J. Lode, C. Lévêque, L. B. Madsen, A. I. Streltsov, and O. E. Alon, Colloquium: Multiconfigurational time-dependent hartree approaches for indistinguishable particles, *Rev. Mod. Phys.* **92**, 011001 (2020).
- [18] D. Hochstuhl and M. Bonitz, Two-photon ionization of helium studied with the multiconfigurational time-dependent Hartree-Fock method, *The Journal of Chemical Physics* **134**, 084106 (2011), https://pubs.aip.org/aip/jcp/article-pdf/doi/10.1063/1.3553176/14905108/084106_1_online.pdf.
- [19] D. Hochstuhl and M. Bonitz, Time-dependent restricted-active-space configuration-interaction method for the photoionization of many-electron atoms, *Phys. Rev. A* **86**, 053424 (2012).
- [20] T. Sato and K. L. Ishikawa, Time-dependent complete-active-space self-consistent-field method for multielectron dynamics in intense laser fields, *Phys. Rev. A* **88**, 023402 (2013).
- [21] A. J. Daley, C. Kollath, U. Schollwöck, and G. Vidal, Time-dependent density-matrix renormalization-group using adaptive effective hilbert spaces, *Journal of Statistical Mechanics: Theory and Experiment* **2004**, P04005 (2004).
- [22] M. Zvolak and G. Vidal, Mixed-state dynamics in one-dimensional quantum lattice systems: A time-dependent superoperator renormalization algorithm, *Phys. Rev. Lett.* **93**, 207205 (2004).
- [23] U. Schollwöck, The density-matrix renormalization group in the age of matrix product states, *Annals of Physics* **326**, 96 (2011), january 2011 Special Issue.
- [24] U. Schollwöck, The density-matrix renormalization group, *Rev. Mod. Phys.* **77**, 259 (2005).
- [25] T. D. Crawford and H. F. Schaefer, An Introduction to Coupled Cluster Theory for Computational Chemists, in *Reviews in Computational Chemistry*, edited by K. B. Lipkowitz and D. B. Boyd (John Wiley & Sons, Inc., 2000) pp. 33–136.
- [26] R. J. Bartlett and M. Musiał, Coupled-cluster theory in quantum chemistry, *Rev. Mod. Phys.* **79**, 291 (2007).
- [27] G. Wälz, D. Kats, D. Usvyat, T. Korona, and M. Schütz, Application of Hermitian time-dependent coupled-cluster response Ansatz of second order to excitation energies and frequency-dependent dipole polarizabilities, *Phys. Rev. A* **86**, 052519 (2012).
- [28] L. N. Koulias, D. B. Williams-Young, D. R. Nascimento, A. E. I. DePrince, and X. Li, Relativistic Real-Time Time-Dependent Equation-of-Motion Coupled-Cluster, *J. Chem. Theory Comput.* **15**, 6617 (2019).
- [29] A. S. Skeidsvoll, A. Balbi, and H. Koch, Time-dependent coupled-cluster theory for ultrafast transient-absorption spectroscopy, *Phys. Rev. A* **102**, 023115 (2020).
- [30] A. S. Skeidsvoll and H. Koch, Comparing real-time coupled-cluster methods through simulation of collective Rabi oscillations, *Phys. Rev. A* **108**, 033116 (2023).

- [31] S. Kvaal, Ab initio quantum dynamics using coupled-cluster, *J. Chem. Phys.* **136**, 194109 (2012).
- [32] T. Sato, H. Pathak, Y. Orimo, and K. L. Ishikawa, Communication: Time-dependent optimized coupled-cluster method for multielectron dynamics, *J. Chem. Phys.* **148**, 051101 (2018).
- [33] H. Pathak, T. Sato, and K. L. Ishikawa, Time-dependent optimized coupled-cluster method for multielectron dynamics. II. A coupled electron-pair approximation, *The Journal of Chemical Physics* **152**, 124115 (2020).
- [34] R. Peng, A. F. White, H. Zhai, and G. Kin-Lic Chan, Conservation laws in coupled cluster dynamics at finite temperature, *The Journal of Chemical Physics* **155**, 044103 (2021).
- [35] L. Reining, The *GW* approximation: content, successes and limitations, *WIREs Computational Molecular Science* **8**, e1344 (2018).
- [36] G. Onida, L. Reining, and A. Rubio, Electronic excitations: density-functional versus many-body green's-function approaches, *Rev. Mod. Phys.* **74**, 601 (2002).
- [37] W. G. Aulbur, L. Jönsson, and J. W. Wilkins, Quasiparticle calculations in solids, *Journal of Physics C: Solid State Physics* **54**, 1 (2000).
- [38] R. Martin, L. Reining, and D. Ceperley, *Interacting Electrons* (Cambridge University Press, 2016).
- [39] J. Wilhelm, P. Seewald, and D. Golze, Low-scaling gw with benchmark accuracy and application to phosphorene nanosheets, *Journal of Chemical Theory and Computation* **17**, 1662 (2021), pMID: 33621085, <https://doi.org/10.1021/acs.jctc.0c01282>.
- [40] D. Neuhauser, Y. Gao, C. Arntsen, C. Karshenas, E. Rabani, and R. Baer, Breaking the Theoretical Scaling Limit for Predicting Quasiparticle Energies: The Stochastic *GW* Approach, *Phys. Rev. Lett.* **113**, 076402 (2014).
- [41] V. Vlček, W. Li, R. Baer, E. Rabani, and D. Neuhauser, Swift *GW* beyond 10,000 electrons using sparse stochastic compression, *Phys. Rev. B* **98**, 075107 (2018).
- [42] W. Gao, W. Xia, X. Gao, and P. Zhang, Speeding up gw calculations to meet the challenge of large scale quasiparticle predictions, *Scientific Reports* **6**, 36849 (2016).
- [43] M. Govoni and G. Galli, Large scale gw calculations, *Journal of Chemical Theory and Computation* **11**, 2680 (2015), pMID: 26575564, <https://doi.org/10.1021/ct500958p>.
- [44] L. Hedin, New method for calculating the one-particle green's function with application to the electron-gas problem, *Phys. Rev.* **139**, A796 (1965).
- [45] V. Vlček, Stochastic vertex corrections: Linear scaling methods for accurate quasiparticle energies, *Journal of chemical theory and computation* **15**, 6254 (2019).
- [46] C. Mejuto-Zaera and V. Vlček, Self-consistency in *GW*T formalism leading to quasiparticle-quasiparticle couplings, *Phys. Rev. B* **106**, 165129 (2022).
- [47] G. Stefanucci and R. van Leeuwen, *Nonequilibrium Many-Body Theory of Quantum Systems: A Modern Introduction* (Cambridge University Press, 2013).
- [48] L. Kadanoff and G. Baym, *Quantum Statistical Mechanics* (The Benjamin/Cummings Publishing Company, New York, 1961).
- [49] J. Schwinger, Brownian Motion of a Quantum Oscillator, *Journal of Mathematical Physics* **2**, 407 (1961), https://pubs.aip.org/aip/jmp/article-pdf/2/3/407/19046507/407_1.online.pdf.
- [50] M. Bonitz, *Quantum Kinetic Theory* (Springer International Publishing Switzerland, 2015).
- [51] J. Kaye and D. Golež, Low rank compression in the numerical solution of the nonequilibrium Dyson equation, *SciPost Phys.* **10**, 091 (2021).
- [52] J. Kaye and H. U. R. Strand, A fast time domain solver for the equilibrium Dyson equation, *Advances in Computational Mathematics* **49**, 10.1007/s10444-023-10067-7 (2023).
- [53] J. Yin, Y.-h. Chan, F. da Jornada, D. Qiu, C. Yang, and S. G. Louie, Analyzing and predicting non-equilibrium many-body dynamics via dynamic mode decomposition, *arXiv preprint arXiv:2107.09635* (2021).
- [54] C. Stahl, N. Dasari, J. Li, A. Picano, P. Werner, and M. Eckstein, Memory truncated Kadanoff-Baym equations, *Phys. Rev. B* **105**, 115146 (2022).
- [55] P. Lipavský, V. Špička, and B. Velický, Generalized Kadanoff-Baym ansatz for deriving quantum transport equations, *Phys. Rev. B* **34**, 6933 (1986).
- [56] N. Schlünzen, J.-P. Joost, and M. Bonitz, Achieving the Scaling Limit for Nonequilibrium Green Functions Simulations, *Phys. Rev. Lett.* **124**, 076601 (2020).
- [57] C. C. Reeves, J. Yin, Y. Zhu, K. Z. Ibrahim, C. Yang, and V. Vlček, Dynamic mode decomposition for extrapolating nonequilibrium Green's-function dynamics, *Phys. Rev. B* **107**, 075107 (2023).
- [58] C. C. Reeves, Y. Zhu, C. Yang, and V. Vlček, Unimportance of memory for the time nonlocal components of the kadanoff-baym equations, *Phys. Rev. B* **108**, 115152 (2023).
- [59] N. Schlünzen, J.-P. Joost, F. Heidrich-Meisner, and M. Bonitz, Nonequilibrium dynamics in the one-dimensional Fermi-Hubbard model: Comparison of the nonequilibrium Green-functions approach and the density matrix renormalization group method, *Phys. Rev. B* **95**, 165139 (2017).
- [60] M. Bonitz, S. Hermanns, and K. Balzer, Dynamics of Hubbard Nano-Clusters Following Strong Excitation, *Contributions to Plasma Physics* **53**, 778 (2013).
- [61] K. Balzer, S. Hermanns, and M. Bonitz, The generalized Kadanoff-Baym ansatz. Computing nonlinear response properties of finite systems, *Journal of Physics: Conference Series* **427**, 012006 (2013).
- [62] S. Hermanns, K. Balzer, and M. Bonitz, Few-particle quantum dynamics—comparing nonequilibrium Green functions with the generalized Kadanoff–Baym ansatz to density operator theory, *Journal of Physics: Conference Series* **427**, 012008 (2013).
- [63] M. P. von Friesen, C. Verdozzi, and C.-O. Almbladh, Artificial damping in the Kadanoff-Baym dynamics of small Hubbard chains, *Journal of Physics: Conference Series* **220**, 012016 (2010).
- [64] M. P. von Friesen, C. Verdozzi, and C.-O. Almbladh, Successes and Failures of Kadanoff-Baym Dynamics in Hubbard Nanoclusters, *Phys. Rev. Lett.* **103**, 176404 (2009).
- [65] See Supplemental Material at for technical details on each of the methods employed in this paper, as well as the relevant implementation details. Additional results are also included: Comparison of methods in a long range interacting model, asymptotic behaviour of the equilibrium natural occupations with increasing U and analysis of the system entropy with different system sizes.
- [66] T. J. Park and J. C. Light, Unitary quantum time evolution by iterative Lanczos reduction, *J. Chem. Phys.* **85**,

- 5870 (1986).
- [67] A. Stan, N. Dahlen, and R. van Leeuwen, Time propagation of the Kadanoff–Baym equations for inhomogeneous systems, *J. Chem. Phys.* **130**, 224101 (2009).
- [68] M. S. Hybertsen and S. G. Louie, Electron correlation in semiconductors and insulators: Band gaps and quasiparticle energies, *Physical Review B* **34**, 5390 (1986).
- [69] J.-P. Joost, N. Schlünzen, and M. Bonitz, G1-G2 scheme: Dramatic acceleration of nonequilibrium Green functions simulations within the Hartree-Fock generalized Kadanoff-Baym ansatz, *Phys. Rev. B* **101**, 245101 (2020).
- [70] G. Harsha, T. M. Henderson, and G. E. Scuseria, Thermofield Theory for Finite-Temperature Coupled Cluster, *J. Chem. Theory Comput.* **15**, 6127 (2019).
- [71] S. Yuan, Y. Chang, and L. K. Wagner, Quantification of electron correlation for approximate quantum calculations, *The Journal of Chemical Physics* **157**, 194101 (2022), https://pubs.aip.org/aip/jcp/article-pdf/doi/10.1063/5.0119260/16552862/194101_1_online.pdf.
- [72] C. Reeves and V. Vlcek, A real-time dyson expansion scheme: Efficient inclusion of dynamical correlations in non-equilibrium spectral properties (2024), [arXiv:2403.07155](https://arxiv.org/abs/2403.07155) [physics.comp-ph].